

Measuring anion binding at biomembrane interfaces

Received: 5 May 2022

Accepted: 29 July 2022

Published online: 08 August 2022

Check for updates

Xin Wu¹, Patrick Wang¹, William Lewis¹, Yun-Bao Jiang² & Philip A. Gale¹✉

The quantification of anion binding by molecular receptors within lipid bilayers remains challenging. Here we measure anion binding in lipid bilayers by creating a fluorescent macrocycle featuring a strong sulfate affinity. We find the determinants of anion binding in lipid bilayers to be different from those expected that govern anion binding in solution. Charge-dense anions H_2PO_4^- and Cl^- that prevail in dimethyl sulfoxide fail to bind to the macrocycle in lipids. In stark contrast, ClO_4^- and Γ^- that hardly bind in dimethyl sulfoxide show surprisingly significant affinities for the macrocycle in lipids. We reveal a lipid bilayer anion binding principle that depends on anion polarisability and bilayer penetration depth of complexes leading to unexpected advantages of charge-diffuse anions. These insights enhance our understanding of how biological systems select anions and guide the design of functional molecular systems operating at biomembrane interfaces.

Molecular interactions at biomembrane interfaces^{1,2} are ubiquitous in many biological processes and underpin several mechanisms of drug action^{3–7}. In particular, anion binding to membrane-embedded proteins and transmembrane anion transport facilitated by channels, carriers and pumps regulate the electrochemical gradients of Cl^- , HCO_3^- , and organic anions which are fundamental to biological functions such as cell volume regulation, pH homeostasis, solute transport and neurotransmission. Apart from proteins, a few small-molecule metabolites (e.g., prodigiosin⁸) and several classes of synthetic molecular receptors⁹ that contain electron-deficient anion binding cavities are known to facilitate anion transport across lipid bilayer membranes. These molecules have been proposed as putative therapeutics for ion channel diseases^{3,7} and cancer^{4,6,10}.

Despite the advances in the area of anion receptor chemistry and transmembrane anion transport, fundamental knowledge of anion binding to natural or synthetic molecular receptors within lipid bilayers is lacking¹¹. The majority of anion binding studies of molecular receptors are conducted in organic solvents and occasionally in aqueous solutions^{12–15}, typically by NMR titration techniques. In lipid bilayers, however, difficulties including poor solubility of receptors, signal broadening and weak anion affinities

have so far impeded the application of NMR or other techniques to elucidating anion binding for anion receptors within the membrane environments.

In this work, we have successfully measured the anion binding affinities of a fluorescent macrocycle **1** (Fig. 1a) within lipid bilayers. This highly symmetric macrocycle has a ~ 3.5 Å cavity composed of a perfectly aligned array of nine strong NH hydrogen bond donors pointing inwards. This ensures hydrogen bonding interactions with large anions such as SO_4^{2-} are sufficiently strong to be measurable in lipid bilayer environments, which we have found to be highly competitive. Here we report our discovery that despite the anion binding selectivity pattern of **1** strongly favouring charge-dense anions H_2PO_4^- and Cl^- in dimethyl sulfoxide (DMSO), when embedded within lipid bilayers, **1** demonstrates binding selectivity towards charge-diffuse ClO_4^- and Γ^- anions (among monovalent anions). In lipid bilayers, preferential binding of charge-diffuse anions benefits from their higher polarisabilities and the deeper bilayer penetration of their complexes, the latter evidenced by fluorescence quenching studies using spin-labelled lipids. In comparison, the binding of charge-dense anions is hampered by severe electrostatic screening at the interfacial headgroup region. These findings correlate with the Hofmeister anion transport selectivity

¹School of Chemistry, The University of Sydney, Sydney, NSW 2006, Australia. ²Department of Chemistry, College of Chemistry and Chemical Engineering, The MOE Key Laboratory of Spectrochemical Analysis and Instrumentation, and iChEM, Xiamen University, 361005 Xiamen, China.

✉ e-mail: philip.gale@sydney.edu.au

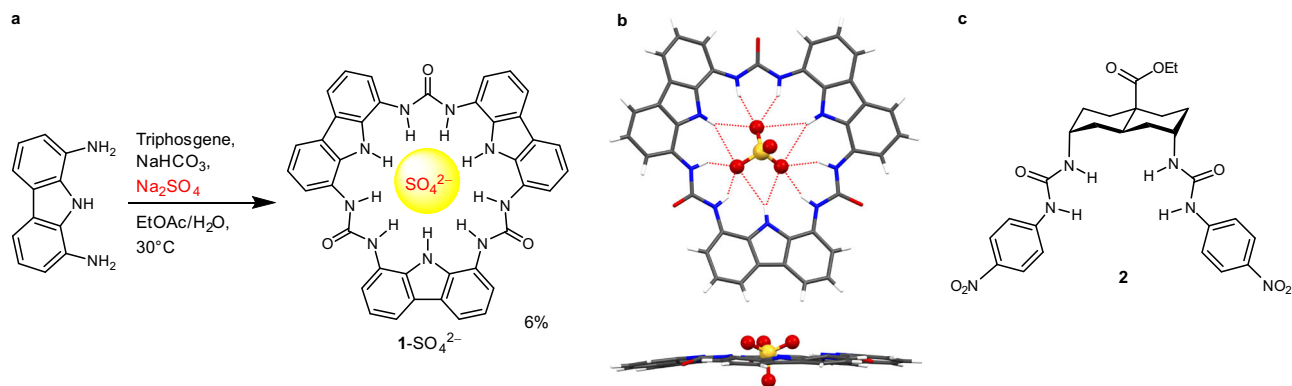


Fig. 1 | Compound structures, synthesis and crystal structure. **a** Synthesis of macrocycle **1**. The SO_4^{2-} template could be removed by EtOAc/ H_2O extraction, which, however, led to partial degradation of the macrocycle. The free macrocycle with 80–90% purity was used in ^1H NMR titrations in $\text{DMSO-}d_6/0.5\%$ H_2O . The pure SO_4^{2-} complex was used in fluorescence and membrane transport studies in water

where the complex completely dissociated at 50 nM due to the competitive aqueous conditions. **b** Top and side views of the crystal structure of the $\mathbf{1-SO}_4^{2-}$ complex (CCDC: 2128483) with solvent removed by PLATON SQUEEZE and cation and disorder omitted for clarity. **c** Reference bis-urea anion receptor **2**.

Table 1 | Anion binding and transmembrane anion transport properties of compound 1, along with literature values of anion hydration free energies and anion binding properties of compound 2 and PC vesicles

Anion	ΔG_{hydr} (kJ mol^{-1}) ^a	Association constant K_a (M^{-1})				Transport rate by $\mathbf{1}/\text{anions s}^{-1}\text{carrier}^{-1}$ ^f	
		In $\text{DMSO-}d_6/0.5\%$ H_2O		In C12E8 micelles	In POPC vesicles		
		1	2 ^b	1	1		
SO_4^{2-}	-975	$(7.4 \pm 1.1) \times 10^9$	$>10^5$	$54,000 \pm 3000$	370 ± 10^c	ND	0.042 ± 0.006
H_2PO_4^-	-473	$>10^5$	46,000	140 ± 20	<1	ND	0.031 ± 0.010
Cl^-	-344	2000 ± 100	670	19 ± 1^c	<1	0.2^d	0.082 ± 0.016
Br^-	-318	200 ± 10	70	29 ± 1^c	2.6 ± 0.6^c	2^d	0.097 ± 0.018
NO_3^-	-286	340 ± 10	10	210 ± 10^c	24 ± 4^c	2.8^d	2.1 ± 0.1
I^-	-280	6.1 ± 0.6	3	200 ± 10^c	24 ± 2^c	32^e	2.0 ± 0.4
ClO_4^-	-229	<1	ND	32 ± 1^c	45 ± 9^c	115^e	0.83 ± 0.10

Errors represent SD from at least two experiments.

ND not determined.

^aGibbs energies of hydration at 25 °C, compiled by Marcus²⁵.

^bReported by Jurček et al.²⁰.

^cIonic strength fixed at 0.2 M.

^dReported by Tatulian³⁴, using egg PC vesicles.

^eReported by Rydall and Macdonald³³, using POPC vesicles.

^fDetermined at an anion concentration of 20 mM.

pattern typically observed for carrier-mediated transmembrane anion transport.

Results and discussion

Synthesis and crystal structure of macrocycle 1

The structure of trimeric carbazole-urea macrocycle **1** was initially proposed in a theoretical study in 2017¹⁶, but no synthetic progress was subsequently made despite the reported synthesis of the dimeric¹⁷ and the tetrameric¹⁸ analogues. We have developed a remarkably simple one-pot SO_4^{2-} -templated synthesis to access the uniquely flat and pre-organised trimeric macrocycle **1** (Fig. 1a). We obtained the crystal structure of the $\mathbf{1-SO}_4^{2-}$ (Fig. 1b) complex modelled with severely disordered solvent molecules removed by PLATON SQUEEZE. The complex shows D_{3d} symmetry with a centrally bound SO_4^{2-} ion forming six strong hydrogen bonds with the three urea units of **1** and additional stabilisation of the complex by six longer carbazole $\text{NH}\cdots\text{SO}_4^{2-}$ hydrogen bonds. The macrocycle was slightly buckled (Fig. 1b right) to accommodate the large tetrahedral SO_4^{2-} ion. Despite the limitation that the solvent molecules including those surrounding the cation could not be modelled, the crystal structure confirms the ability of **1** to bind a SO_4^{2-} ion within its central cavity via multiple hydrogen bonds in the solid state.

Anion binding in DMSO, micelles and lipid bilayers

We conducted ^1H NMR titrations of **1** with tetrabutylammonium (TBA^+) salts of SO_4^{2-} , H_2PO_4^- , Cl^- , Br^- , NO_3^- , I^- and ClO_4^- in $\text{DMSO-}d_6/0.5\%$ H_2O (Table 1). Both SO_4^{2-} (Fig. 2a) and H_2PO_4^- (Supplementary Fig. 14) lead to slow exchange ^1H NMR responses, which were rarely observed¹⁹ in the relatively competitive organic solvent DMSO highlighting the anion binding potency of **1**. By contrast, the complexes of **1** with Cl^- , Br^- , NO_3^- and I^- show fast exchange with the free macrocycle (Supplementary Figs. 5–12). The addition of ClO_4^- even at >100 mM induced no discernible ^1H chemical shift changes of **1** (Supplementary Fig. 13).

Macrocycle **1** has an exceptionally strong SO_4^{2-} affinity in the sub-nanomolar range, which necessitates the use of a BaSO_4 precipitation method for quantification. For monovalent anions, the anion binding affinity decreases in the order of $\text{H}_2\text{PO}_4^- > \text{Cl}^- > \text{NO}_3^- > \text{Br}^- > \text{I}^- > \text{ClO}_4^-$ (Table 1). Compared with Davis's acyclic bis-urea **2** (Fig. 1c)²⁰, the macrocyclic receptor confers a modest 1–2 fold affinity enhancement for Cl^- , Br^- and I^- , but a significant 33-fold enhancement for NO_3^- . Geometrical optimisation of the anion complexes is evidence in support of the hypothesis that **1** has the perfect size and shape complementary fit for NO_3^- resulting in a precisely flat and D_{3h} -symmetric complex (Supplementary Fig. 4b)¹⁶. By contrast, the macrocyclic cavity

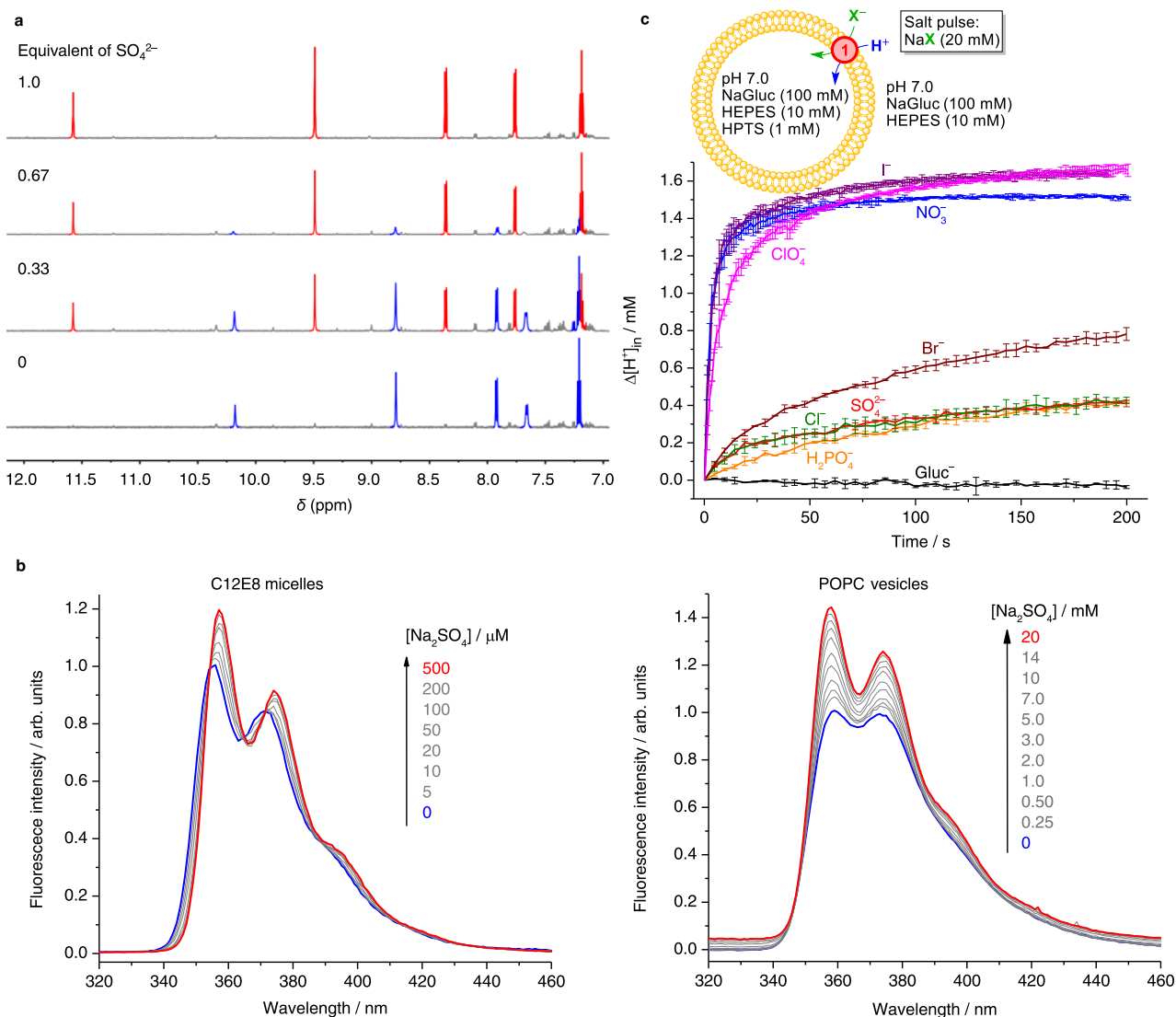


Fig. 2 | Anion binding and transmembrane anion transport by macrocycle 1. **a** ^1H NMR (600 MHz) titration of **1** (0.3 mM) with TBA_2SO_4 in $\text{DMSO}-d_6/0.5\% \text{H}_2\text{O}$. Signals from free **1** and the 1-SO_4^{2-} complex are shown in blue and red, respectively. Impurities are present from partial degradation of **1** during SO_4^{2-} removal. **b** Fluorescence titration of **1** (50 nM) with Na_2SO_4 in C12E8 (2 mM) micelles (left) and POPC (0.2 mM) vesicles (right) in H_2O . $\lambda_{\text{ex}} = 265 \text{ nm}$. **c** Transmembrane H^+/X^-

symport (influx) facilitated by **1** (1 mol%) upon the external addition of a NaX (20 mM) salt in NaGluc vesicles buffered at pH 7.0 with 10 mM HEPES. Error bars represent SD from two experiments. C12E8 octaethylene glycol monododecyl ether, POPC 1-palmitoyl-2-oleoyl-sn-glycero-3-phosphocholine, NaGluc sodium gluconate, HEPES 4-(2-hydroxyethyl)-1-piperazineethanesulfonic acid, HPTS 8-hydroxypyrene-1,3,6-trisulfonate.

is slightly too large for I^- (Supplementary Fig. 4c) and consequently much too large for Br^- (Supplementary Fig. 4d) and Cl^- (Supplementary Fig. 4e). Notably, here without using **2** as a reference receptor for comparison, the macrocycle's structural preference for NO_3^- would have been lost in the binding constant data in DMSO, as charge-dense²¹ monovalent anions H_2PO_4^- and Cl^- have much greater affinities than NO_3^- which only narrowly edges out Br^- . Thus, in DMSO the anion binding affinities of **1** are dominated by the strength of electrostatic interactions leading to favourable binding of charge-dense anions. Interestingly, for a recently reported hexapodal cage that binds anions via less acidic alkyl amide NH and imine CH sites¹⁹, a weaker $\text{SO}_4^{2-}/\text{I}^-$ selectivity of ~ 30 and a $\text{I}^- > \text{Cl}^-$ selectivity were found in $\text{DMSO}-d_6$ contrasting the behaviour of macrocycle **1** that binds anion via highly acidic aromatic urea and carbazole NH sites. This suggests that the extent of preference for charge-dense anions is influenced by the acidity of anion binding sites.

To evaluate the anion binding strength of **1** in water, we next switched the medium from DMSO to non-ionic octaethyleneglycol

monododecyl (C12E8, Fig. 3b left) micelles dispersed in water²², as neither **1** nor its anion complex is soluble in pure water. Macrocycle **1** can be solubilised at sub- μM concentrations in C12E8 micelles and demonstrates a fluorescence enhancement response to SO_4^{2-} (Fig. 2b), giving a remarkable SO_4^{2-} binding constant of $5.4 \times 10^4 \text{ M}^{-1}$ in water.

Apart from H_2PO_4^- that induced a fluorescence response similar to SO_4^{2-} (Supplementary Fig. 19), other anions produced either negligible fluorescence responses (Cl^-) or fluorescence quenching responses (Br^- , NO_3^- , I^- and ClO_4^-) partly attributable to dynamic quenching (Supplementary Fig. 21), rendering direct fluorescence titrations unfeasible. Instead, we conducted competition titrations with SO_4^{2-} in the presence of these anions and calculated the affinities based on the attenuation of SO_4^{2-} affinity using a competition binding model. In these analyses, it was necessary to correct the binding constant values against Boltzmann factors as anions adsorb to micellar surfaces²³ leading to a negative surface potential (estimated by electrophoretic measurements) which then reduces the SO_4^{2-} concentration at the surface by a Boltzmann factor compared within the bulk solution.

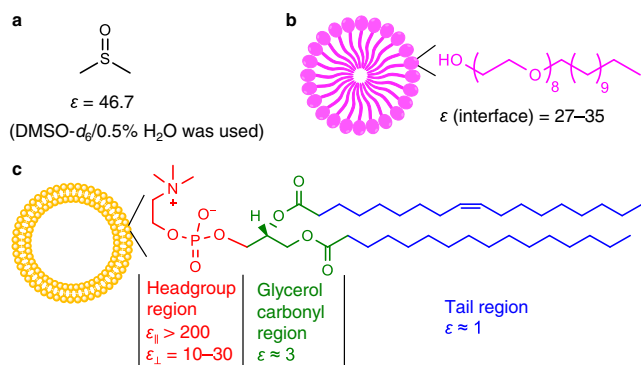


Fig. 3 | Dielectric properties of three media used for anion binding studies in this paper. **a** DMSO. **b** C12E8 micelles, where the interfacial dielectric constant was determined by Drummond et al.²⁴ based on pK_a shifts of lipoidal pH indicators. **c** POPC vesicles with theoretically modelled dielectric constants. The dielectric constants of the headgroup region were taken from Stern & Feller²⁸ and Raudino & Mauzerall²⁹, and the values of the remaining regions from Nymeyer & Zhou²⁷.

Table 1 demonstrates a modified anion selectivity in water/C12E8 compared with in DMSO, despite SO_4^{2-} remaining as the most strongly bound anion. While H_2PO_4^- , Cl^- and NO_3^- are the top-3 strongest binding monovalent anions in DMSO, Cl^- drops out of this group in the water/C12E8 system and is replaced by Γ^- . We rationalise the binding data on the basis of anion solvation free energies and medium polarity (Fig. 3). The interfacial dielectric constant of C12E8 micelles was estimated to be $\sim 27\text{--}35$ ²⁴, which is similar to that of MeCN and lower than DMSO, and hence anion binding should not be weakened solely on medium polarity considerations. Here the diminished affinities of charge-dense SO_4^{2-} , H_2PO_4^- and Cl^- anions, and the shift of anion selectivity towards more charge-diffuse NO_3^- and Γ^- anions are attributed to the heavier dehydration costs of charge-dense than charge-diffuse anions²⁵. The augmented affinities of Γ^- and ClO_4^- in water/C12E8 than in DMSO despite the anion dehydration cost in water/C12E8 can be rationalised by the high receptor desolvation cost in DMSO (see Supplementary Fig. 11 for evidence of desolvation)¹⁴. We have also performed ^1H NMR of macrocycle **1** in water/C12E8 in the presence of anions (Supplementary Fig. 29), in which the observation of resonances from anion complexes provided unambiguous evidence of binding of all tested anions in the biphasic system.

Importantly, macrocycle **1** also demonstrated a fluorescence enhancement response to SO_4^{2-} (Fig. 2b right) when incorporated at sub- μM concentrations in POPC (Fig. 3c) vesicles suspended in water. A further reduced SO_4^{2-} affinity of 370 M^{-1} was found for **1** in POPC vesicles compared with in C12E8 micelles (Table 1). This attenuation could be in part due to competitive receptor binding to the phosphate headgroup of POPC²⁶. To gain more evidence for this, we performed SO_4^{2-} titrations of **1** in 10% and 20% POPC/C12E8 mixed micelles, which demonstrated 4.5-fold and 9-fold reduced SO_4^{2-} affinities (Supplementary Figs. 19 and 20), respectively, compared with in pure C12E8 micelles. Further evidence was provided by direct observation of ^1H NMR signals corresponding to the **1**-POPC complex in POPC/C12E8 mixed micelles (Supplementary Fig. 30).

Examination of binding constants of other anions in POPC vesicles (determined by competition binding experiments with surface potential effects corrected, Table 1) has however revealed a trend that cannot be explained solely by competitive headgroup binding which does not impact anion selectivity. Strikingly, while the divalent SO_4^{2-} always remained the strongest binding anion, the top-three monovalent anion group changed again compared to C12E8 micelles, with H_2PO_4^- being knocked out by ClO_4^- which joins NO_3^- and Γ^- . In POPC vesicles, H_2PO_4^- and Cl^- no longer showed appreciable affinities ($K_a < 1\text{ M}^{-1}$). This trend also cannot be explained by anion dehydration costs alone, as anion binding is subject to the dehydration requirement

in both water/C12E8 and water/POPC systems. The dielectric property of the lipid bilayers, on the other hand, could provide a clue to understanding the enhanced selectivity for charge-diffuse anions in POPC vesicles than in C12E8 micelles. Previously molecular dynamics simulation studies have estimated the dielectric constant of the zwitterionic headgroup region to be higher than that of bulk water ($\epsilon_{||} > 200$, where $\epsilon_{||}$ is the dielectric constant component parallel to the bilayer surface and affects half of the NH-binding sites on average assuming perpendicular insertion of the macrocycle; the perpendicular component ϵ_{\perp} was estimated to be $\sim 10\text{--}30$, which affects the remaining half of the NH sites)^{27–29}. Flood and coworkers have shown in a Cl^- -binding macrocycle that with a higher solvent dielectric constant, the energetic contribution of electrostatic interactions reduces while non-electrostatic induction and dispersion contributions start to dominate¹³. Thus the reason that should anion binding occur at the high dielectric constant headgroup region, charge-dense anions SO_4^{2-} , H_2PO_4^- and Cl^- that mainly rely on electrostatic interactions to bind would be disadvantaged over large charge-diffuse anions ClO_4^- and Γ^- that have favourable induction and dispersion terms due to their polarisabilities. This effect would add to the chaotropic preference that arises from dehydration cost alone as we have already seen in C12E8 micelles.

Location of macrocycle **1** in lipid bilayers

Key information on the location of anion binding in POPC vesicles was then obtained by fluorescence penetration-depth studies using spin-labelled lipids to quench the fluorescence of **1** at different locations (Supplementary Figs. 43–46)³⁰. Without anions, the most probable location of macrocycle **1** was determined to be 19 \AA from the bilayer centre, corresponding to the headgroup region. This is consistent with the hypothesis that free anion receptors can bind to the phosphate headgroup of lipids²⁶. Macrocycle **1** remains at the headgroup region upon binding to SO_4^{2-} , but upon binding to ClO_4^- penetrates deeper (16 \AA) into the carbonyl/glycerol region with a lower dielectric constant of $3\text{--}4$ ²⁷. Here we have confirmed that the binding of SO_4^{2-} occurs at the high dielectric constant headgroup region, supporting the hypothesis that the binding of charge-dense anions is subject to severe electrostatic screening which diminishes their affinities (note that the SO_4^{2-} selectivity persists but is much weaker than in DMSO and in C12E8 micelles). We have shown an additional benefit for charge-diffuse anions such as ClO_4^- that their complexes (and likely also the free anions^{31,32}) can penetrate deeper into a more hydrophobic microenvironment where anion binding is enhanced.

It is of interest to compare the anion binding properties of macrocycle **1** in lipids against anion binding by lipids themselves. Lipid bilayers preferentially adsorb charge-diffuse anions and exhibit a Hofmeister selectivity pattern of $\text{ClO}_4^- > \Gamma^- > \text{NO}_3^- > \text{Br}^- > \text{Cl}^- > \text{H}_2\text{PO}_4^-$ (see also Supplementary Table 3)^{33,34}. Table 1 shows that macrocycle **1** binds Br^- , Γ^- and ClO_4^- with similar or weaker affinities than lipids, but binds NO_3^- ~ 8 times more strongly than lipids, again manifesting the perfect size and shape matching of the macrocycle for NO_3^- (Supplementary Fig. 3b). The ability of lipids to preferentially accumulate ClO_4^- below the headgroup region^{31,32}, on the other hand, has overwhelmed the macrocycle's preference for NO_3^- .

Further information came to light when we compare the above-mentioned phenomena to cation binding to lipids and to the cation receptor/carrier valinomycin in lipids. The cation affinities of PC lipids among alkali metal cations from Li^+ to Rb^+ are very similar³⁵, while being far weaker than lipids binding charge-diffuse anions^{33,34}. For valinomycin, although cation binding affinities dropped by several orders of magnitude when the medium switched from organic solvents to lipids, no drastic alteration of cation selectivity was found in lipids³⁶ in contrast to the behaviour of “anti-valinomycin” **1**. As shown by previous theoretical investigations, the greater polarisability of large charge-diffuse anions³⁷ is central to their strong interfacial

adsorption^{38,39} and in the cases of water/lipid interfaces, this then benefits anion binding to an anion receptor embedded in lipids due to increased local anion concentrations, in addition to highly polarisable anions having favourable induction and dispersion interactions with an anion receptor. This effect is absent in cation binding because of the poor polarisabilities of cations.

Transmembrane anion transport by macrocycle **1**

Finally, to gain a better understanding of the biomedically relevant topic of carrier-mediated anion transport^{4,6,7,9,10} based on our current findings, we studied macrocycle **1** as an anion transporter in POPC vesicles (Fig. 2c)⁴⁰. Macrocycle **1** functions as an H⁺/anion⁻ symporter but not as an anion uniporter (Supplementary Fig. 50) presumably due to the strong headgroup binding that inhibited transmembrane diffusion of the free receptor²⁶. An anion transport selectivity of NO₃⁻ ≈ I⁻ > ClO₄⁻ > Br⁻ > Cl⁻ > SO₄²⁻ > H₂PO₄⁻ was observed by initial rate comparison (Table 1, Fig. 2c), which correlates with, but is not identical to the anion binding selectivity in lipids. Carrier-mediated ion transport rates depend both on the ion binding affinity and the rate of ion-carrier complex diffusion through the membrane⁴¹, the latter being unfavourable for the doubly charged SO₄²⁻. While NO₃⁻ and I⁻ can be fully embedded into the macrocyclic plane (Supplementary Fig. 4b, c), ClO₄⁻ has an exposed oxygen atom after binding to **1** (Supplementary Fig. 4a), likely slowing down ClO₄⁻ transport than the transport of NO₃⁻ and I⁻. In light of the ClO₄⁻, I⁻ > NO₃⁻ transport selectivity commonly observed for structurally simple hydrogen bond-based anion transporters following Hofmeister series⁴², here the clear NO₃⁻ > ClO₄⁻ transport selectivity of **1** again reflects macrocycle's structural fit for NO₃⁻, which, however, is insufficient to confer a significant NO₃⁻ > I⁻ selectivity due to the preference of the lipid environment for the more hydrophobic I⁻. Our results in lipid bilayers thus explain the difficulty⁴² of overcoming the Hofmeister bias to facilitate selective membrane transport of more hydrophilic anions such as Cl⁻ which shows a deceptively strong affinity of 2000 M⁻¹ for **1** in DMSO. In addition, as high-efficacy anion transporters typically have Cl⁻ affinities in the range of 10²–10⁴ M⁻¹ in DMSO⁷, our results imply that those systems likely bind Cl⁻ with low affinities of <10 M⁻¹ in lipid bilayers and hence should operate far from ion binding saturation when transporting Cl⁻ under physiologically relevant conditions.

In summary, we have gained access to the intricacies of anion binding at biomembrane interfaces taking advantage of a strong SO₄²⁻ binding macrocycle **1** showing fluorescence perturbation upon binding SO₄²⁻ at interfaces. We show that in organic solvents such as DMSO, electrostatic effects dominate leading to preferential binding of charge-dense anions. In biphasic systems with a moderate interfacial polarity such as non-ionic micelles, both electrostatic and dehydration effects operate such that a range of anions across the Hofmeister scale can bind. Contrastingly, we show that anion binding in lipid bilayers behaves differently from the above two scenarios in that anion polarisability, electrostatic screening and penetration depth underlie anion binding strength/selectivity leading to surprisingly favourable binding of charge-diffuse anions, in particular, ClO₄⁻. In all tested media, we have seen the intrinsic size/shape matching selectivity of **1** for NO₃⁻ struggling to manifest itself amid the electrostatic, solvation and polarisability effects characteristic of the anions and medium conditions. The elucidation of anion binding principles at lipid bilayers is important to diverse research topics ranging from ion interactions with membrane-embedded proteins/peptides to the development of drug delivery vehicles and synthetic receptors/transporters/assemblies functioning at biomembrane interfaces.

Methods

General

All reagents were purchased from commercial sources and used as received. NMR spectra were recorded on a Bruker Avance III 400 NMR

Spectrometer equipped with a BBFO room temperature probe or a Bruker Avance III 600 NMR Spectrometer equipped with a TCI cryoprobe. High-resolution mass spectra (HRMS) were recorded on a Bruker Apex Qe 7 T Fourier Transform Ion Cyclotron Resonance Mass Spectrometer. Inductively coupled plasma mass spectrometry (ICP-MS) was acquired on a Perkin Elmer Nexion 350X Inductively Coupled Plasma Mass Spectrometer. Fluorescence studies were performed on a Horiba Fluoromax-4 or an Agilent Cary Eclipse Fluorescence Spectrometer equipped with a magnetic stirrer and a temperature controller. Dynamic light scattering (DLS) and electrophoretic mobility measurements were performed on a Malvern Zetasizer Nano ZS. Single crystal X-ray diffraction was performed on a Bruker APEX-II CCD diffractometer.

¹H NMR titrations in DMSO-*d*₆/0.5% H₂O

A DMSO-*d*₆ stock solution of free macrocycle **1** was diluted to 0.3 mM in 0.5 mL of DMSO-*d*₆/0.5% H₂O. The solution was titrated against TBA⁺ salts of anions and the ¹H NMR spectra were acquired. The chemical shifts of the NH and CH resonances were plotted against the anion concentration and the data were fitted to a suitable binding model (1:1 or 1:2 host-guest) to determine the binding constants. For SO₄²⁻, a competition BaSO₄ precipitation method was used due to strong binding. See Supplementary Information for details.

Fluorescence titrations in C12E8 micelles and POPC vesicles

A DMSO stock solution of **1**-SO₄²⁻ complex (10 μM) was diluted to 50 nM in 2.5 mL of H₂O containing C12E8 (2 mM) micelles or POPC (0.2 mM) vesicles, the latter extruded with 100 nm polycarbonate membranes. The solution was titrated against Na₂SO₄ and the fluorescence spectra were recorded. The fluorescence intensity at 357 nm (in C12E8 micelles) or 358 nm (in POPC vesicles) was plotted against the anion concentration and fitted to a 1:1 binding model to calculate the SO₄²⁻ binding constant.

For both systems (C12E8 micelles and POPC vesicles), the SO₄²⁻ titration was also performed in the presence of a competing anion (as a Na⁺ salt, with the ionic strength fixed at 0.2 M) to indirectly determine the binding constant of the competing anion using a competition binding model. The zeta potentials of C12E8 micelles and POPC vesicles in the presence of the competing anion were determined by electrophoretic measurements, from which the surface potential values were estimated based on the Gouy-Chapman model⁴³. The Boltzmann factor for SO₄²⁻ calculated from the surface potential value was used to correct the binding data against the surface potential effect. See Supplementary Information for details.

Transmembrane anion transport

A “salt-pulse” assay was used to determine the rate of H⁺/anion symport facilitated by macrocycle **1**. A DMSO solution of **1**-SO₄²⁻ complex (final concentration 1 μM) was added to a suspension of POPC (0.1 mM) vesicles (diameter ~200 nm) loaded with and suspended in sodium gluconate (NaGluc, 100 mM) buffered at pH 7.0 with HEPES (10 mM). NaX (20 mM, X⁻ = Gluc⁻, H₂PO₄⁻, Cl⁻, Br⁻, NO₃⁻, I⁻ or ClO₄⁻) or Na₂SO₄ (20 mM) was added to the vesicle suspension. H⁺/anion symport facilitated by macrocycle **1** leads to intra-vesicular acidification monitored by an intra-vesicular fluorescence pH indicator HPTS. The fluorescence data were converted to H⁺ influx (Δ[H]_{in}) as detailed in Supplementary Information.

Data availability

Data supporting the findings of this study are available from the manuscript and its supplementary information. Supplementary Data File 1 contains the xyz coordinates for the optimised structures. Files containing the raw data have been deposited in figshare with the <https://doi.org/10.6084/m9.figshare.20155097> accession code. The crystal structure of **1**-SO₄²⁻ complex has been deposited at the

Cambridge Crystallographic Data Centre (CCDC), under deposition number 2128483. These data can be obtained free of charge from The Cambridge Crystallographic Data Centre via www.ccdc.cam.ac.uk/data_request/cif.

References

- Langton, M. J. Engineering of stimuli-responsive lipid-bilayer membranes using supramolecular systems. *Nat. Rev. Chem.* **5**, 46–61 (2021).
- Gonella, G. et al. Water at charged interfaces. *Nat. Rev. Chem.* **5**, 466–485 (2021).
- Muraglia, K. A. et al. Small-molecule ion channels increase host defences in cystic fibrosis airway epithelia. *Nature* **567**, 405–408 (2019).
- Park, S.-H. et al. Determinants of ion-transporter cancer cell death. *Chem* **5**, 2079–2098 (2019).
- Kaushik, V., Yakisich, J. S., Kumar, A., Azad, N. & Iyer, A. K. V. Ionophores: potential use as anticancer drugs and chemosensitizers. *Cancers* **10**, 360 (2018).
- Busschaert, N. et al. A synthetic ion transporter that disrupts autophagy and induces apoptosis by perturbing cellular chloride concentrations. *Nat. Chem.* **9**, 667–675 (2017).
- Li, H. et al. Efficient, non-toxic anion transport by synthetic carriers in cells and epithelia. *Nat. Chem.* **8**, 24–32 (2016).
- Fürstner, A. Chemistry and biology of roseophilin and the prodigiosin alkaloids: a survey of the last 2500 years. *Angew. Chem. Int. Ed.* **42**, 3582–3603 (2003).
- Davis, J. T., Gale, P. A. & Quesada, R. Advances in anion transport and supramolecular medicinal chemistry. *Chem. Soc. Rev.* **49**, 6056–6086 (2020).
- Ko, S.-K. et al. Synthetic ion transporters can induce apoptosis by facilitating chloride anion transport into cells. *Nat. Chem.* **6**, 885–892 (2014).
- Cremer, P. S., Flood, A. H., Gibb, B. C. & Mobley, D. L. Collaborative routes to clarifying the murky waters of aqueous supramolecular chemistry. *Nat. Chem.* **10**, 8 (2017).
- Fiala, T., Sleziaikova, K., Marsalek, K., Salvadori, K. & Sindelar, V. Thermodynamics of halide binding to a neutral bambusuril in water and organic solvents. *J. Org. Chem.* **83**, 1903–1912 (2018).
- Liu, Y., Sengupta, A., Raghavachari, K. & Flood, A. H. Anion binding in solution: beyond the electrostatic regime. *Chem* **3**, 411–427 (2017).
- Sommer, F., Marcus, Y. & Kubik, S. Effects of solvent properties on the anion binding of neutral water-soluble bis(cyclopeptides) in water and aqueous solvent mixtures. *ACS Omega* **2**, 3669–3680 (2017).
- Busschaert, N., Caltagirone, C., Van Rossom, W. & Gale, P. A. Applications of supramolecular anion recognition. *Chem. Rev.* **115**, 8038–8155 (2015).
- Bauzá, A., Frontera, A. & Mooibroek, T. J. NO₃⁻ anions can act as Lewis acid in the solid state. *Nat. Commun.* **8**, 14522 (2017).
- Ahmed, N., Geronimo, I., Hwang, I.-C., Singh, N. J. & Kim, K. S. Cyclo-bis(urea-3,6-dichlorocarbazole) as a chromogenic and fluorogenic receptor for anions and a selective sensor of zinc and copper cations. *Chem. Eur. J.* **17**, 8542–8548 (2011).
- Rüütel, A. et al. Design, synthesis and application of carbazole macrocycles in anion sensors. *Beilstein J. Org. Chem.* **16**, 1901–1914 (2020).
- Xie, H., Gunawardana, V. W. L., Finnegan, T. J., Xie, W. & Badjić, J. D. Picking on carbonate: kinetic selectivity in the encapsulation of anions. *Angew. Chem. Int. Ed.* **61**, e202116518 (2022).
- Jurček, O. et al. Anion recognition by a bioactive diureidodecalin anionophore: solid-state, solution, and computational studies. *Chem. Eur. J.* **24**, 8178–8185 (2018).
- Pike, S. J., Hutchinson, J. J. & Hunter, C. A. H-bond acceptor parameters for anions. *J. Am. Chem. Soc.* **139**, 6700–6706 (2017).
- Keymeulen, F. et al. Fluoride binding in water with the use of micellar nanodevices based on salophen complexes. *Org. Biomol. Chem.* **13**, 2437–2443 (2015).
- Murgia, S., Monduzzi, M. & Palazzo, G. Quantification of specific anion binding to non-ionic Triton X-100 micelles. *Langmuir* **28**, 1283–1289 (2012).
- Drummond, C. J., Warr, G. G., Grieser, F., Ninham, B. W. & Evans, D. F. Surface properties and micellar interfacial microenvironment of *n*-dodecyl β-D-maltoside. *J. Phys. Chem.* **89**, 2103–2109 (1985).
- Marcus, Y. in *Ions in Solution and their Solvation* (ed Marcus, Y.) 107–155 (Wiley, 2015).
- Wu, X. et al. Voltage-switchable HCl transport enabled by lipid headgroup–transporter interactions. *Angew. Chem. Int. Ed.* **58**, 15142–15147 (2019).
- Nymeyer, H. & Zhou, H.-X. A method to determine dielectric constants in nonhomogeneous systems: application to biological membranes. *Biophys. J.* **94**, 1185–1193 (2008).
- Stern, H. A. & Feller, S. E. Calculation of the dielectric permittivity profile for a nonuniform system: application to a lipid bilayer simulation. *J. Chem. Phys.* **118**, 3401–3412 (2003).
- Raudino, A. & Mauzerall, D. Dielectric properties of the polar head group region of zwitterionic lipid bilayers. *Biophys. J.* **50**, 441–449 (1986).
- Kondo, M., Mehiri, M. & Regen, S. L. Viewing membrane-bound molecular umbrellas by parallax analyses. *J. Am. Chem. Soc.* **130**, 13771–13777 (2008).
- Sachs, J. N. & Woolf, T. B. Understanding the Hofmeister effect in interactions between chaotropic anions and lipid bilayers: molecular dynamics simulations. *J. Am. Chem. Soc.* **125**, 8742–8743 (2003).
- Clarke, R. J. & Lüpfer, C. Influence of anions and cations on the dipole potential of phosphatidylcholine vesicles: a basis for the Hofmeister effect. *Biophys. J.* **76**, 2614–2624 (1999).
- Rydall, J. R. & Macdonald, P. M. Investigation of anion binding to neutral lipid membranes using deuterium NMR. *Biochemistry* **31**, 1092–1099 (1992).
- Tatulian, S. A. Binding of alkaline-earth metal cations and some anions to phosphatidylcholine liposomes. *Eur. J. Biochem.* **170**, 413–420 (1987).
- Klasczyk, B., Knecht, V., Lipowsky, R. & Dimova, R. Interactions of alkali metal chlorides with phosphatidylcholine vesicles. *Langmuir* **26**, 18951–18958 (2010).
- Meers, P. & Feigenson, G. W. Location and ion-binding of membrane-associated valinomycin, a proton nuclear magnetic resonance study. *Biochim. Biophys. Acta.* **938**, 469–482 (1988).
- Assaf, K. I. & Nau, W. M. The chaotropic effect as an assembly motif in chemistry. *Angew. Chem. Int. Ed.* **57**, 13968–13981 (2018).
- Son, C. Y. & Wang, Z.-G. Image-charge effects on ion adsorption near aqueous interfaces. *Proc. Natl Acad. Sci. USA* **118**, e2020615118 (2021).
- Jungwirth, P. & Tobias, D. J. Ions at the air/water interface. *J. Phys. Chem. B* **106**, 6361–6373 (2002).
- Matile, S. & Sakai, N. in *Analytical Methods in Supramolecular Chemistry* (ed Schalley, C. A.) 711–742 (Wiley-VCH, 2012).
- Läuger, P. Carrier-mediated ion transport: electrical relaxation experiments give insight into the kinetics of ion transport through artificial lipid membrane. *Science* **178**, 24–30 (1972).
- Wu, X. & Gale, P. A. Measuring anion transport selectivity: a cautionary tale. *Chem. Commun.* **57**, 3979–3982 (2021).
- Eisenberg, M., Gresalfi, T., Riccio, T. & McLaughlin, S. Adsorption of monovalent cations to bilayer membranes containing negative phospholipids. *Biochemistry* **18**, 5213–5223 (1979).

Acknowledgements

X.W., P.W., W.L. and P.A.G. acknowledge and pay respect to the Gadigal people of the Eora Nation, the traditional owners of the land on which we research, teach and collaborate at the University of Sydney. We thank the Australian Research Council (DP210100039, P.A.G. and DE220101000, X.W.), the National Natural Science Foundation of China (21820102006, Y.B.J. and P.A.G.) and the University of Sydney for funding. We thank Prof Eric Ross (Gonzaga University) for helpful discussions, and Dr. Nicholas Proschogo and Jakob D. Lane (The University of Sydney) for performing HRMS and ICP-MS.

Author contributions

X.W. and P.A.G. conceived the project and X.W. carried out the synthesis and analytical studies. P.W. contributed to the synthetic work. W.L. conducted the crystallographic studies. P.A.G., Y.B.J. and X.W. obtained the funding for the project. P.A.G. supervised and directed the research. The manuscript was written by X.W. and revised by P.A.G. and Y.B.J.

Competing interests

The authors declare no competing interests.

Additional information

Supplementary information The online version contains

supplementary material available at <https://doi.org/10.1038/s41467-022-32403-z>.

Correspondence and requests for materials should be addressed to Philip A. Gale.

Peer review information *Nature Communications* thanks Eduardo Escudero-Adán, Mihail Barboiu and the other, anonymous, reviewer(s) for their contribution to the peer review of this work.

Reprints and permission information is available at <http://www.nature.com/reprints>

Publisher's note Springer Nature remains neutral with regard to jurisdictional claims in published maps and institutional affiliations.

Open Access This article is licensed under a Creative Commons Attribution 4.0 International License, which permits use, sharing, adaptation, distribution and reproduction in any medium or format, as long as you give appropriate credit to the original author(s) and the source, provide a link to the Creative Commons license, and indicate if changes were made. The images or other third party material in this article are included in the article's Creative Commons license, unless indicated otherwise in a credit line to the material. If material is not included in the article's Creative Commons license and your intended use is not permitted by statutory regulation or exceeds the permitted use, you will need to obtain permission directly from the copyright holder. To view a copy of this license, visit <http://creativecommons.org/licenses/by/4.0/>.

© The Author(s) 2022